Aerodynamic Forces on Finite Wings in Oscillatory Flow: An Experimental Study

M. H. Patel*
University College London, London, England

This report describes aerodynamic lift and pitching moment measurements on finite wings in oscillating vertical gusts of varying frequency parameter and gust amplitude. A set of six conventional wings with varying aspect ratio, sweep angle, and taper are tested. The results show that the variation of aerodynamic force per unit gust amplitude with frequency parameter is independent of freestream velocity, wing incidence, and gust amplitude but is considerably influenced by wing sweep. These experimental results are compared with a lifting surface theory for two of the test planforms and show good agreement. The effect on the aerodynamic forces of allowing free transition on the wing surfaces is also investigated.

Nomenclature

x,y,z = Cartesian frame of reference ("wind axes") shown in Fig. 5
$\bar{x}$ = nondimensionalized x coordinate ($=x/c$)
t = time coordinate
A = wing aspect ratio
C_L = lift coefficient ($=L/\frac{1}{2}\rho U^2 S$)
C_m = pitching moment coefficient about a line through the root quarter chord point ($=M/\frac{1}{2}\rho U^2 Sc$)
c = geometric mean wing chord
L = lift force
M = pitching moment about a line through the root quarter chord point
S = wing area in plan
U = mean freestream velocity
w = instantaneous vertical (downwash) velocity component of gust
$\bar{w}$ = instantaneous angle of incident gust ($=w/U$)
w_g = amplitude of vertical (downwash) velocity component in oscillatory flow
$\bar{w}_g$ = amplitude of incident gust angle in oscillatory flow (w_g/U)
α = angle of incidence of test wing—positive nose down about y axis (Fig. 5)
ΔC_L = amplitude of lift coefficient in oscillatory flow ($=\Delta L/\frac{1}{2}\rho U^2 S$)
ΔC_m = amplitude of pitching moment coefficient about a line through the root quarter chord point ($=\Delta M/\frac{1}{2}\rho U^2 Sc$)
ΔL = amplitude of lift in oscillating flow
ΔM = amplitude of pitching moment about a line through the root quarter chord point
$\Lambda_{1/4}$ = sweep angle of wing quarter chord line
λ = wing taper ratio (= tip chord/root chord)
ν = frequency parameter ($=\omega c/U$)
ν' = "effective" frequency parameter ($=\omega c/0.61U$)
ρ = air density
ω = radian frequency

Introduction

THE response of aircraft to atmospheric turbulence is of significant current interest with particular regard to the design of active control systems for which aerodynamic loads due to turbulence are a major perturbing influence during operation. At present, theoretical predictions of wing loads in atmospheric turbulent conditions are based on modeling both the continuous gusts and the aircraft response by superposition of harmonic components. To contribute to the understanding of loads on a wing due to oscillatory gusts, without the attendant aircraft response, the characteristics of various wing planforms have been measured in a known simple harmonic vertical gust. One of the primary aims of the present work is to obtain a comprehensive set of experimental data for comparison with several available theoretical methods which model the oscillating flow around finite wings.[1] Such experimental data for aerodynamic forces on finite wings in irrotational gusts are virtually nonexistent, although some related investigations[2-4] have been made for two dimensional airfoils. On the other hand, the aerodynamic problem of the oscillating lifting surface in steady flow has been extensively studied.[1,5]

In this investigation, lift and pitching moment measurements have been made on a set of six wings in oscillatory gusts. Their planform shapes are designated by letters A to F and are as follows: 1) wings A, B, and E are untapered wings of aspect ratio 6 with sweeps of 0, 22.5, and 45 deg, respectively; 2) wing D is a tapered wing of aspect ratio 6 with a taper ratio of 0.5 deg and 22.5 deg quarter chord line sweep; 3) wing C is an untapered wing of aspect ratio 8 and a sweep of 22.5 deg; 4) wing F is an untapered wing of aspect ratio 4 and a sweep of 45 deg.

Gust Tunnel Facility

The gust tunnel used for these tests has been described fully by Patel and Hancock.[6] It is based on a conventional wind tunnel with a rigid semiopen working section made up of solid vertical sidewalls and an essentially open top and bottom. The gust generation device, shown in Fig. 1, consists of flexible extensions to the top and bottom walls at the exit to the contraction. These upper and lower extensions are fixed at their ends to a frame which can be moved up and down. Fixed sidewalls extend the contraction exit to the frame. Oscillatory motion of the frame by an electro-hydraulic servo-mechanism perturbs the shear layers above and below the semiopen test section into rolling up and forming discrete vortices in the jet mixing regions. The systems of rolled up vortices convect downstream with a velocity of 0.61 of the mean freestream velocity and induce an oscillatory traveling waveform of irrotational vertical gust in the working section, which can be written mathematically as

$$\bar{w}(x,t) = \bar{w}_g(x)\, e^{i\omega[t+(x/0.61U)]} \qquad (1)$$

Received Dec. 15, 1977; revision received Aug. 3, 1978.

Index category: Nonsteady Aerodynamics.

*Lecturer, Dept. of Mechanical Engineering. Member AIAA.

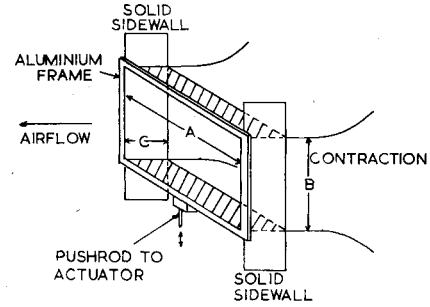

Fig. 1 The flexible nozzle. Shaded areas are flexible walls. A = 0.99 m, B = 0.76 m and C = 0.38 m.

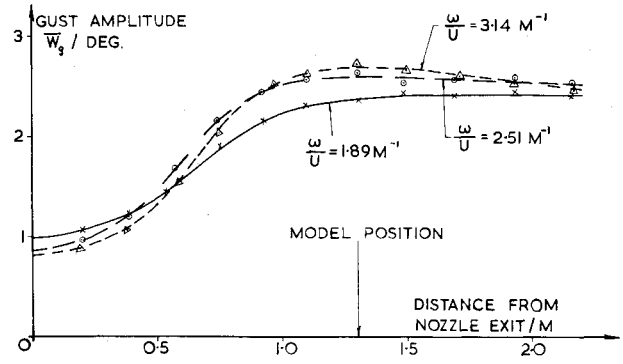

Fig. 2 Oscillatory gust amplitude variation with downstream distance.

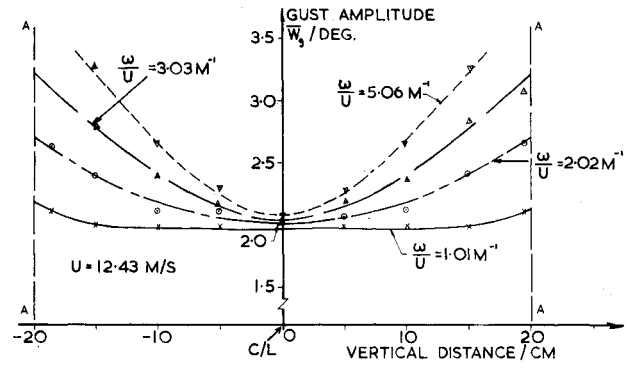

Fig. 3 Oscillatory gust amplitude variation with vertical distance. Lines AA denote approximate mixing region boundaries.

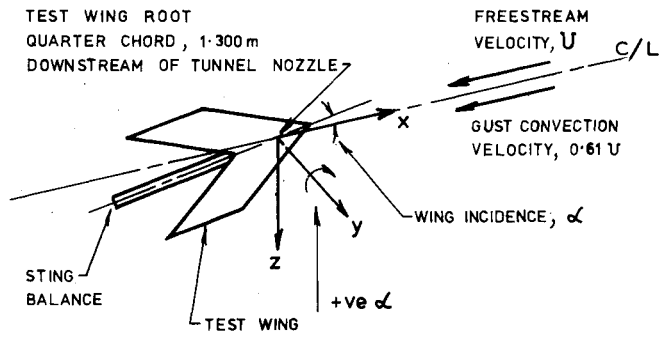

Fig. 4 The wing reference axes system. Incidence, α defined as nose-down positive.

where $0.61U$ is the velocity of the traveling wave convecting downstream.

The usable frequency range, written in terms of frequency parameter per unit chord (in m) is $1.01 < \omega/U < 5.06$ for a gust amplitude of $\bar{w}_g = 0.0314$, or 1.8 deg gust incidence angle. For a frequency parameter of around $\omega/U = 2.2$ m^{-1}, gust amplitudes of up to $\bar{w}_g = 0.054$ ($\simeq 3.1$ deg) are available. The actual frequencies corresponding to these frequency parameters lie in the range from 2 to 12 Hz.

The spatial distribution of gust amplitude in the working section is important for the determination of the size and position of the test models. Figure 2 illustrates typical variations of gust amplitude with downstream distance aft of the nozzle. For a model positioned 1.300 m aft of the nozzle, a region of constant gust amplitude is available for the wing and its wake. The wake is in this region of constant gust amplitude up to the end of the working section sidewalls which are 1.300 m downstream of the model position. Figure 3 shows typical variations of gust amplitude with vertical distance from the working section centerline. The "hyperbolic cosine" variation of vertical velocity is due to the presence of vortex streets above and below the test section which induce the required unsteady flow. This feature, however, is not in itself a limitation. The main restriction is the available height of irrotational flow between the upper and lower mixing regions; which as seen from Fig. 3 is ±20 cm about the centerline and is more than adequate for the thin wings used in these tests.

Measurements of the oscillatory flow in the spanwise direction across the working section confirm a closely two-dimensional gust. In view of the preceding considerations, the test wings were positioned such that their root quarter chord points were 1.300 m downstream of the nozzle on the working section centerline.

Models and Test Equipment

The two considerations which governed the choice of planform shapes to be tested were, first, the need to test as wide a range of commonly used wing shapes as possible and, second, the desirability of wing planforms which could be easily modeled by theoretical methods. For the latter reason, all the wings had straight leading and trailing edges as well as wing root sting mountings which were enclosed within the wing thickness so as to provide a wing only configuration without any center body at the root. All the wings were of NACA 0010 aerofoil section with rounded streamwise tips. Planform sizes were determined by fixing a leading dimension, the span, to 0.60 m which is 60% of the working section width. Figure 4 shows the reference "wind" axes system. Positive incidence is taken to be nose down to insure consistency of "positive" lift with either wing incidence or downward gust velocity.

Aerodynamic forces on the wings were measured by a cantilever-type lift and pitching moment sensing sting balance. The balance was designed for very low strain levels and of minimum length in order to maximize the natural frequency of bending vibrations. Adequate sensitivity was maintained by the use of semiconductor strain gages with a high gage factor (~180) and a negligible level of gage factor drift due to temperature (~0.022% per °C), using internal compensation.

The effects on the mesurements of oscillatory deflections of the sting under oscillating aerodynamic loads were calculated.[7] The magnitude of the resulting measurement error was shown to be extremely small due to the combination of high sting stiffness and the small aerodynamic loads that were involved. The accuracy of the measurements was, however, affected by the sting-wing system behaving as a dynamical system with a natural frequency in bending of 60 Hz. A measured dynamic calibration of each sting-wing system required the amplitudes of the oscillating lifts to be corrected by up to about 2% at the highest test frequency (~12 Hz). The low damping present in the system produced negligible phase errors.

The upstream incidence angle and resultant wing force output were recorded by a digital system that sampled the signal to be measured at selected time intervals over successive

oscillation cycles. The upstream incidence, used as a reference, supplied the information for selecting the sampling time instants. The resulting data were a set of "phase averages" which described the measured signal in relation to the reference signal. The phase average is defined as the average value of the measured signal over several successive cycles that is obtained at a particular phase of the reference signal wave cycle. A numerical harmonic analysis of the data sets was performed at the forcing frequency in the reference gust incidence angle. The final results were obtained as amplitude and phase angles of $\Delta C_L/\bar{w}_g$ and $\Delta C_m/\bar{w}_g$ against frequency parameter, $\omega c/U$ within an experimental uncertainty of $\pm 3\%$ in amplitude values and $\pm 2\%$ for phase angles.

Experimental Results

Both the steady and oscillatory flow test were performed for all the wings at two mean freestream velocities of 12.43 and 20.00 m/s. A persistent difficulty in these experiments has been the adequate provision of transition, which was provoked by the use of surface roughness in the form of silicon carbide abrasive paper with a grain height of 0.4 mm and a chordwise extent of up to 10% chord. The roughness strips were mounted 7% of chord aft of the leading edge and parallel to it.

In the absence of surface roughness for provoking transition, the ± 1.8 deg incidence change through an oscillation period either caused the wing surface flow to switch between laminar and turbulent regimes through each cycle or at best it caused the transition region to oscillate back and forth over a substantial part of the chord. As a result, the measured lifts and moments were not consistent with data at other incidences and freestream velocities as they were for the tests with transition fixed just aft of the leading edge. These comments are illustrated by the oscillatory flow mesasurements with free transition that are described subsequently.

An indication of the effect of surface roughness on the wing boundary layer was obtained by the measurement of boundary-layer thickness on the trailing edge at mid-semispan of rectangular wing A. At a freestream velocity of 20.00 m/s, with natural transition, the boundary layer at the trailing edge was turbulent with a thickness of 4.5 mm (4.5% of chord). The transition strips used in these experiments thickened the trailing edge boundary layer slightly to a value of 5.2 mm (5.2% of chord); thus confirming that the roughness strips did not cause excessive boundary-layer thickness changes with none of the consequent effects on the wing aerodynamic forces.

The lift and pitching moment against incidence measurements in steady flow for the six planforms gave the usual results, with linear curves below the stall for both Reynolds numbers due to the effectiveness of the transition strips. The calculated lift and moment curve slopes are incorporated into the oscillatory flow data as values of $\Delta C_L/\bar{w}_g$ and $\Delta C_m/\bar{w}_g$ at zero frequency.

Force measurements in oscillatory flow were made relative to the freestream oscillatory flow at the root quarter chord point. A yawmeter at this point measured the freestream oscillatory gust relative to conditions at an upstream yawmeter. Force measurements were then made for each wing again relative to the upstream yawmeter output. The resulting data are presented as in-phase and out-of-phase components of amplitudes $\Delta C_L/\bar{w}_g$ and $\Delta C_m/\bar{w}_g$ against frequency parameter, $\nu(=\omega c/U)$; where $\bar{w}_g$ is the amplitude of incident gust oscillation at the wing.

A comprehensive range of tests were performed on all of the wings at constant gust amplitudes ($\bar{w}_g \simeq 0.0314$ or 1.8 deg) over a range of frequency parameters ($1.01 < \omega/U < 5.06$, in m^{-1}) at two incidences and two freestream velocities. All the wings were tested at 0-deg incidence as well as a positive incidence chosen to be around 4 deg in order to maintain attached flow at all times together with a turbulent boundary

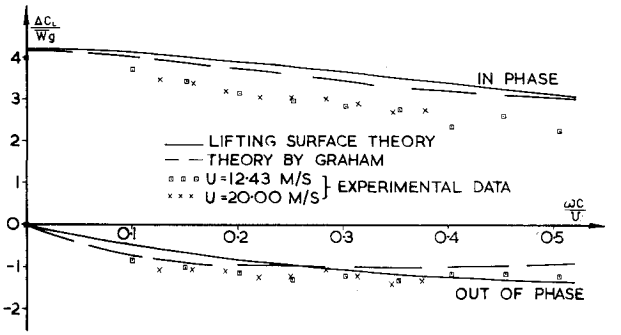

Fig. 5 Comparison between theory and experiment: wing A ($A=6$, $\Lambda_{1/4}=0$ deg, $\lambda=1$) at $\alpha=0$ deg: lift force.

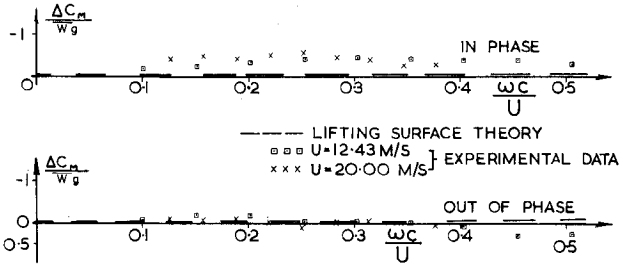

Fig. 6 Comparison between theory and experiment: wing A ($A=6$, $\Lambda_{1/4}=0$ deg, $\lambda=1$) at $\alpha=0$ deg: pitching moment.

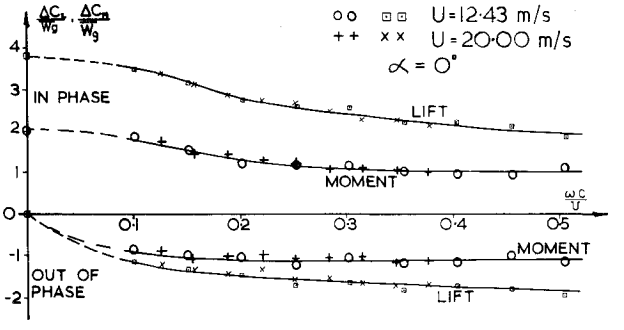

Fig. 7 Wing B ($A=6$, $\Lambda_{1/4}=22.5$ deg, $\lambda=1$) oscillating force measurement.

layer on the wing pressure surface. Measurements were also carried out on all of the wings at constant frequency parameter ($=2.2$ per unit chord), 0-deg incidence and varying gust amplitude, (0.0087 {0.5 deg} $< \bar{w}_g < 0.054$ {3.1 deg}). The results for $\Delta C_L/\bar{w}_g$ variations with gust amplitude for all of the wings showed no significant variations over the range of gust amplitudes used.

Experimental data for lift and pitching moment amplitudes against frequency parameter showed these variations to be independent of wing incidence within the bounds of experimental error. The results for 0-deg wing incidence are plotted in Figs. 5-11 for all of the planforms. The frequency parameter on the abscissae of those curves is expressed in terms of the geometric mean chord, c. Reference 7 gives tabulated data corresponding to the figures shown here.

Figures 5 and 6 show the oscillatory flow results for the rectangular wing A. Important points to note are the close agreement between data at the two freestream velocities, the manner in which the in-phase amplitude curve in lift appears to approach zero frequency parameter, and the magnitude of the lift out-of-phase component, which is equivalent at high frequency parameters to a phase lag of about 23 deg relative to the freestream gust oscillation at the root quarter chord point. The significant variation of pitching moment amplitude with frequency parameter (Fig. 6) is also of interest.

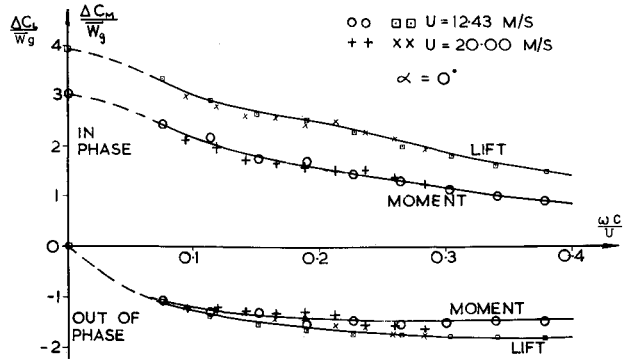

Fig. 8 Wing C ($A = 8$, $\Lambda_{1/4} = 22.5$ deg, $\lambda = 1$) oscillating force measurement.

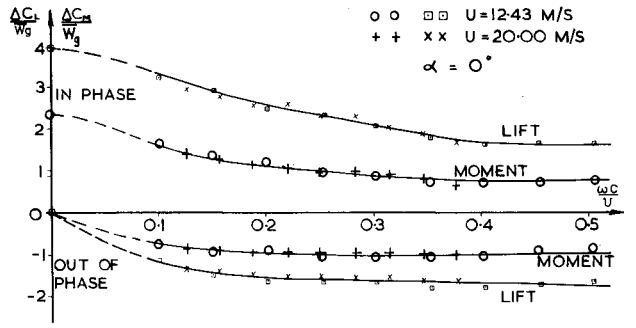

Fig. 9 Wing D ($A = 6$, $\Lambda_{1/4} = 22.5$ deg, $\lambda = 0.5$) oscillating force measurement.

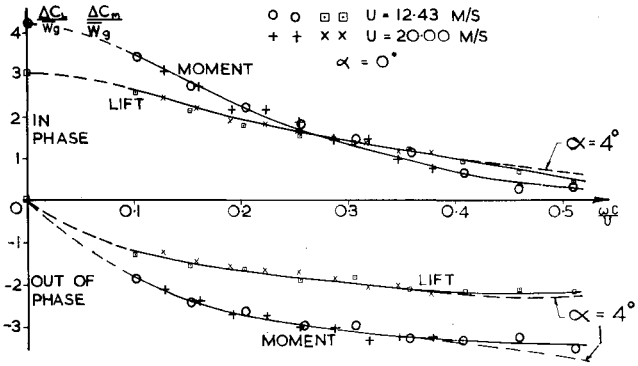

Fig. 10 Wing E ($A = 6$, $\Lambda_{1/4} = 45$ deg, $\lambda = 1$) oscillating force measurement.

Figure 7 displays the results for wing B. In addition to having features already mentioned for wing A, the effect of wing sweep is apparent in the higher out-of-phase components in lift and moment observed here. The amplitude of pitching moment is much larger than in wing A because of the change in aerodynamic center away from the wing root quarter chord point due to wing sweep. The results for wing C (Fig. 8), which is identical to B except for a higher aspect ratio, exhibit no substantial changes due to the aspect ratio increase except for a slight rise in out-of-phase components for both lift and pitching moment. Wing D, the only tapered ($\lambda = 0.5$) wing shows results (Fig. 9) with similar features to those just described. The effect of 22.5 deg wing sweep is observed in the higher out-of-phase components that are obtained here. Wings E and F (Figs. 10 and 11) are both of 45-deg sweep with aspect ratios of 6 and 4, respectively. Oscillatory flow force results for these wings reflect the high angle of sweep in the very large out-of-phase components for both lift force and moment. Apart from this, the comments for the other wings regarding agreement between data at the two freestream

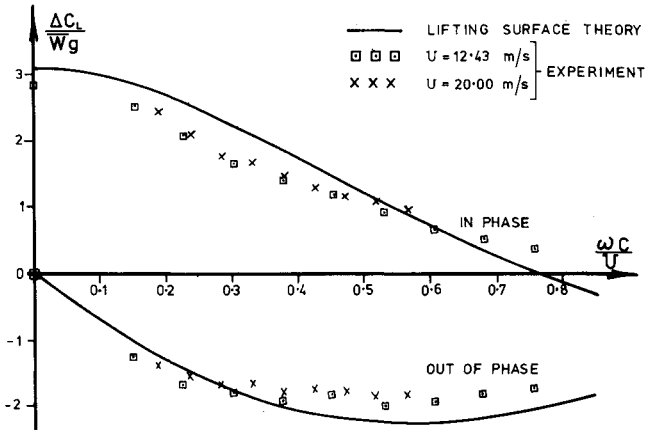

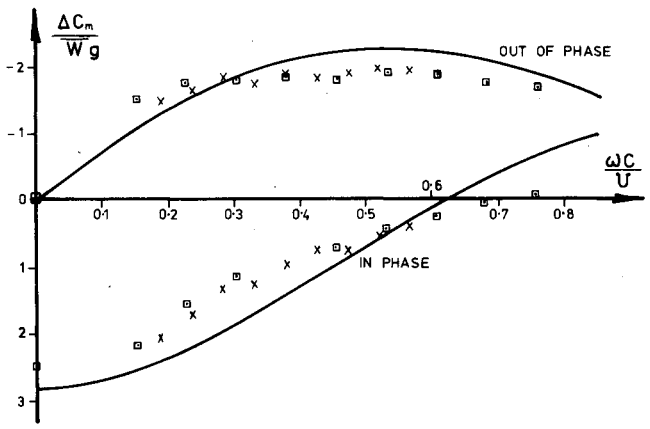

Fig. 11 Comparison between theory and experiment wing F ($A = 4$, $\Lambda_{1/4} = 45$ deg, $\lambda = 1$) at $\alpha = 0$ deg.

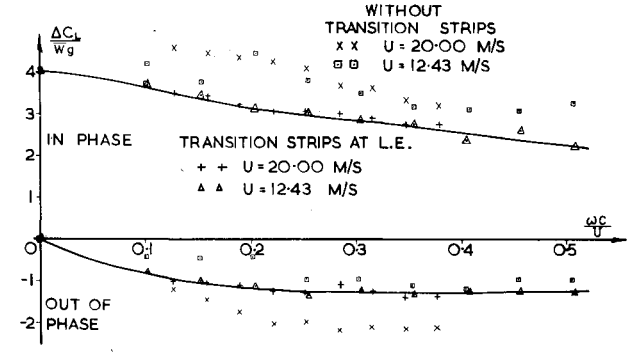

Fig. 12 Wing A ($A = 6$, $\Lambda_{1/4} = 0$ deg, $\lambda = 1$) oscillating lift measurement; effect of transition position for $\alpha = 0$ deg.

velocities and the behavior of the in-phase components in the vicinity of zero frequency apply equally here. In addition, a curious feature observed for wings E and F are the slight discrepancies between data at the two incidences for high frequency parameters; see Fig. 10 for wing E. These are explained subsequently.

Although all of the foregoing tests were performed with transition fixed and the wing leading edge, the effects on the oscillatory lifts and pitching moments of allowing free transition were also explored. Figure 12 displays a comparison between fixed and free transition data for rectangular wing A at 0-deg incidence. The large effect of oscillating free transition on the lift force is apparent here. Figure 13 shows the result at 5-deg incidence; here the discrepancies between fixed and free transition data are not quite as marked because at this nonzero incidence the upper ("suction") wing surface flow has a natural transition region just aft of the leading edge

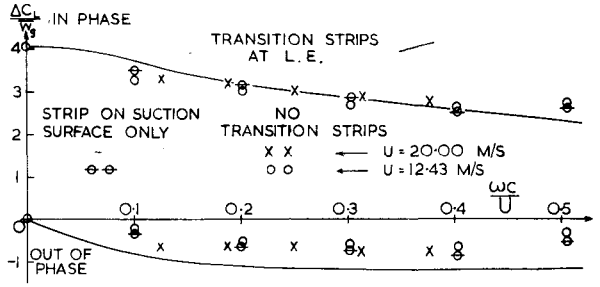

Fig. 13 Wing A ($A=6$, $\Lambda_{1/4}=0$ deg, $\lambda=1$) oscillating lift measurement; effect of transition position for $\alpha=5$ deg.

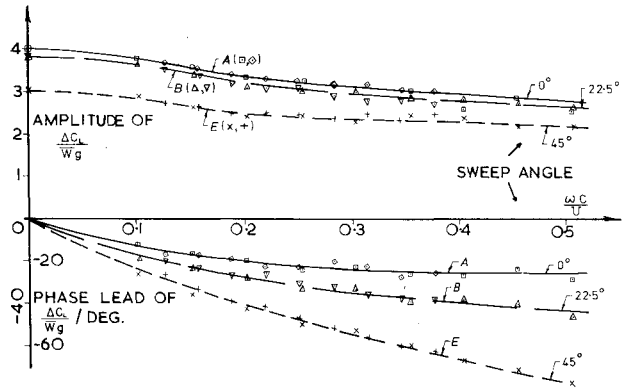

Fig. 14 Oscillating lift measurement: effect of sweep angle for wings A, B, and E, all with $A=6$, $\lambda=1$, $\alpha=0$ deg.

which displays no appreciable periodic chordwise movement due to the oscillatory incidence. This argument is supported by the results of tests (plotted in Fig. 13) with transition fixed on just the suction surface which show no significant departure from the free transition results.

Several tests with varying transition strip thickness have pointed to the fact that the importance of the strips was not so much in provoking transition as in fixing it at a particular chordwise station on the wing surfaces. As long as transition was fixed at a particular station, variation of strip roughness height gave no measurable changes in the force response.

Discussion

It is to be noted that the experiments were done at low Reynolds number (up to 200,000 based on mean geometric chord) with transition strips to simulate the boundary layer at higher Reynolds numbers. No wind tunnel corrections have been applied to the acquired data. The steady flow lift and pitching moment curve slopes are used for the zero frequency case in the oscillatory flow results. These steady flow values were compared with the results of inviscid theory presented in Ref. 8 which is based on the linearized lifting surface theory of Garner and Inch.[9] The agreement was found to be good for all the wings tested.

In considering the oscillatory flow results, a few general points are presented first. Some comparative curves between the various wing measurements have been plotted in terms of the amplitude and phase of lift. Figure 14 shows the influence of wing sweep only for three untapered wings A, B, and E, all of aspect ratio 6 with varying sweep angles of 0, 22.5, and 45 deg, respectively. The substantial rise in phase lag with increasing sweep is well brought out here, although there are no such comparable changes in the lift amplitude. This effect is to be expected since only the phase of the incident gust distribution alters with distance downstream. Figures 15 and 16 display the effect of aspect ratio on the oscillating flow lift response for wing pairs E, F and B, C, respectively. Both comparisons indicate that the phase lag changes for the higher

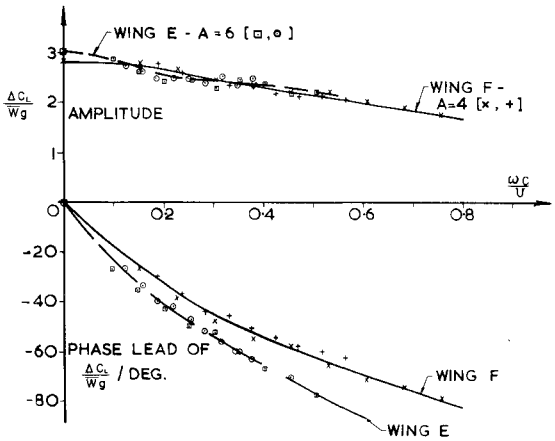

Fig. 15 Oscillating lift measurement: effect of aspect ratio for wings E and F, both with $\lambda=1$, $\Lambda_{1/4}=45$ deg, $\alpha=0$ deg.

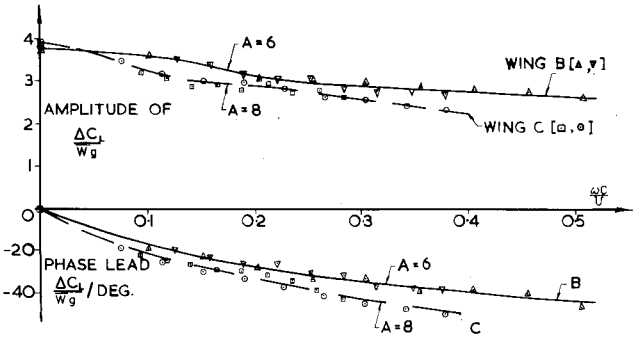

Fig. 16 Oscillating lift measurement: effect of aspect ratio for wings B and C, both with $\lambda=1$, $\Lambda_{1/4}=22.5$ deg, $\alpha=0$ deg.

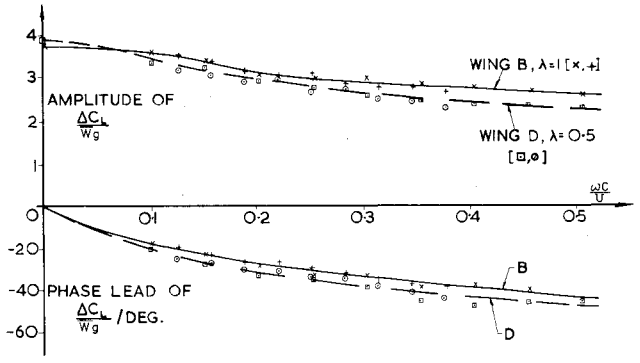

Fig. 17 Oscillating lift measurement: effect of taper for wings B and D, both with $A=6$, $\Lambda_{1/4}=22.5$ deg, $\alpha=0$ deg.

aspect ratio wing are larger. The amplitude variation, however, starts off as larger for the higher aspect ratio wing in steady or very low frequency flow, as would be expected, but then reduces to around the same level or slightly lower than results for the wing of lower aspect ratio. Figure 7 illustrates the effect of taper ratio on the lift response in a similar manner, but no meaningful trend is apparent here.

A characteristic of the force response for wings E and F (45 deg sweep, aspect ratios 6 and 4, respectively) is a distinct difference at high frequency parameters between the results for incidences of 0 and 4 deg. Figure 10 illustrates the difference for wing E. It is caused by the nature of the incident oscillatory flow in the gust tunnel working section. When either wing is at an incidence of 4 deg, its root is on the tunnel centerline while its tips are about 3.2-cm below the centerline. From a description of the tunnel flow characteristics, it is known that at high frequencies, the freestream gust amplitude

between these two points increases by as much as 4% towards the wing tips. The reasoning is confirmed by observing trends in the force response for both wings at 0- and 4-deg incidence at higher frequency parameters.

An important part of the present study is the comparison of acquired experimental data with existing theories. In oscillatory flow, the traveling wave nature of the incident gust has to be accounted for within a theoretical solution of the problem. For the experiments reported here, the gust convection velocity is 0.61 of the freestream velocity. An oscillatory gust which is convecting downstream with the freestream velocity can be expressed mathematically as

$$\bar{w}(x,t) = \bar{w}_g e^{i\omega[t+(x/U)]} \tag{2}$$

Taking $\nu = \omega c/U$ and $\bar{x} = x/c$, gives

$$\bar{w}(x,t) = \bar{w}_g e^{i\nu\bar{x}} e^{i\omega t}$$

where c is the mean geometric chord of a stationary wing in the flowfield. The problem can be solved for the aerodynamic force amplitude per unit gust amplitude ($\bar{w}_g$) in terms of the frequency parameter ν. The oscillatory gust in the test facility can be written as Eq. (1) and transformed to a gust of the form

$$\bar{w}(x,t) = \bar{w}_g e^{(i\nu/0.61)\bar{x}} e^{i\omega t} \tag{3}$$

incident on a stationary wing. This problem is identical to the preceding one except for an effective change of the incident oscillatory gust wavelength. Therefore, comparisons between theories based on a gust moving with the freestream velocity and the present experiments can be made by interpreting the change in wavelengths as specifying an "effective" frequency parameter ν' for the experiments to be

$$\nu' = \frac{\nu}{0.61} = \frac{\omega c}{0.61U} \tag{4}$$

Several theoretical models are currently available for the calculation of oscillatory inviscid flow around finite wings. One of these is lifting surface theory. Computations using this method[10] have been performed for wings A and F (both untapered with aspect ratio 6 and sweeps of 0 and 45 deg, respectively). The calculated results are plotted in Figs. 5, 6, and 11 for comparison with experiment. The agreement is quite good considering the inviscid, thin wing assumptions embodied in the theory. The calculations incorporate the effective frequency parameter required to account for the traveling wave form of the incident oscillatory gust.

Graham[11] describes a method, restricted to rectangular planforms, which utilizes a Fourier transform to solve the downwash integral equation. Results for a wing of aspect ratio 6 are shown plotted with the experimental data in Fig. 5.

Conclusions

The results of this experimental study indicate that forces on finite wings in an oscillating gust environment behave in a predictably consistent manner due to changes in the gust frequency, gust amplitude, and wing incidence, provided that stationary transition is maintained close to the leading edge together with attached flow on the wing surface at all times. Under these conditions, comparisons of experimental data with calculations based on an inviscid lifting surface theory show reasonable agreement.

The shape of wing planform, particularly wing sweep, has a dominant effect on the magnitudes of phase lag variations with frequency parameter. The effects of aspect ratio and taper on the measured forces are observable but not nearly as large.

Acknowledgment

This work was carried out in the Department of Aeronautical Engineering at Queen Mary College, London, with the support of Procurement Executive, Ministry of Defence, U.K.

References

[1] Rodden, W. P., "State of the Art in Unsteady Aerodynamics," AGARD Rept. No. 650, 1976.

[2] Commerford, G. I. and Carta, F. O., "Unsteady Aerodynamic Response of a Two-Dimensional Aerofoil at High Reduced Frequency," *AIAA Journal*, Vol. 12, Jan. 1974, pp. 43-48.

[3] Satyanarayana, B., Gostelow, J. P., and Henderson, R. E., "A Comparison between Experimental and Theoretical Fluctuating Lift on Cascades at Low Frequency Parameters," ASME Paper 74-GT-78, March 1974.

[4] Fujita, H. and Kovasznay, L.S.G., "Unsteady Lift and Radiated Sound from a Wake Cutting Aerofoil," *AIAA Journal*, Vol. 12, Sept. 1974, pp. 1216-1221.

[5] McCroskey, W. J., "Some Current Research in Unsteady Fluid Dynamics," *Journal of Fluids Engineering Transaction of ASME*, Ser. I, March 1977, pp. 8-39.

[6] Patel, M. H. and Hancock, G. J., "A Gust Tunnel Facility," Aeronautical Research Council, London, R&M 3802, 1977.

[7] Patel, M. H., "Lift and Pitching Moment Measurements on Finite Wings in Oscillatory Vertical Gusts," Queen Mary College, London, EP-1022, Sept. 1976.

[8] Engineering Sciences Data Unit Data Sheet, "Lift Curve Slope and Aerodynamic Center Position of Wings in Inviscid Subsonic Flow," Item No. 70011.

[9] Garner, H. C. and Inch, S. M., "Subsonic Theoretical Lift Curve Slope, Aerodynamic Center, and Spanwise Loading for Arbitrary Aspect Ratio, Taper Ratio and Sweepback," National Physical Laboratory, Aero Rept. 1317, May 1970; also Aeronautical Research Council, London, C.P. 1137.

[10] Garner, H. C. and Davies, D. E., private communication.

[11] Graham, J.M.R., "A Lifting Surface Theory for the Rectangular Wing in Non-Stationary Flow," *Aeronautical Quarterly*, Feb. 1971, pp. 83-100.